Low Temperature Physics/Fizika Nizkikh Temperatur, 2021, vol. 47, No. 12, pp. 1165–1172

Biintercalate layered heterostructure: synthesis conditions and physical properties

F. O. Ivashchyshyn[1,3], V. M. Maksymych[1], T. D. Krushelnytska[1], O. V. Rybak[1], B. O. Seredyuk[2], and N. K. Tovstyuk[1]

[1]*Institute of Applied Mathematics and Fundamental Sciences, Lviv Polytechnic National University Lviv 79013, Ukraine*

[2]*Hetman Petro Sahaidachnyi National Army Academy, Lviv 79026, Ukraine*

[3]*Faculty of Electrical Engineering, Czestochowa University of Technology, Częstochowa 42-200, Poland*
E-mail*:* nataliia.k.tovstiuk@lpnu.ua

Received June 29, 2021, published online October 25, 2021

The biintercalation of the layered GaSe semiconductor is carried out by ferroelectric and ferromagnetic guest components. Due to the separation of guest components, the GaSe<$NaNO_2$+$FeCl_3$ nanohybrid has a spatial-scale hybridity, which is due to the alternation of nanoscale regions of one phase with meso- or microdimensions of another. The results of electrical conductivity studies by impedance spectroscopy indicate a 250-fold increase after biintercalation of the GaSe single crystal, due to delocalized current carriers. Confirmation of a significant change in the impurity energy spectrum after biintercalation was obtained by the method of thermally stimulated discharge — GaSe nanohybrid <$NaNO_2$+$FeCl_3$> is characterized by a quasi-continuous spectrum in the entire temperature range of measurements and relaxation of the heterocharge. The GaSe<$NaNO_2$+$FeCl_3$> nano-hybrid is characterized by a high dielectric constant while a tangent of the dielectric loss angle is less than 1 in the high-frequency region of the spectrum. That opens the prospect of its use for the manufacture of high-quality radio-frequency capacitors. Changes in the impurity energy spectrum are investigated for low temperatures in the virtual crystal model, taking into account the Fivazov dispersion law both for the conductivity band and for the two impurity bands. The appearance of an additional gap in the spectrum of impurity states is established and its shift is investigated depending on the concentration of intercalants of different nature — intercalant-acceptor type and donor.

Keywords: biintercalation, layered crystal, nanoscale, nanohybrid, virtual model.

Introduction

The formation of functional materials at the level of nanoscale objects is a powerful tool for purposeful alteration of their properties, and it often provides the ability to obtain extraordinary effects and phenomena. Studies of nanostructured materials with the structural element dimensions in the nanometer range reveal completely new properties and approaches in material science and the study of substances. Materials with anisotropy of physical properties are of great interest to researchers. Such materials include layered crystals of the A^3B^6 group (InSe, GaSe), which allow researchers to search for unique (2D) electronic properties such as high electron mobility, quantum Hall effect, anomalous optical response, or induced zero-resistance states [1, 2].

Due to the peculiarities of the structure, layered crystals of A^3B^6 group are potential thermoelectric materials with high PF (power efficiency) [3], they can be used in various fields of electronics [4, 5] and can serve as matrices with 2D guest positions. “Construction” on their basis of certain inorganic/organic nanostructures by intercalation crystal engineering allows, on the one hand, to expand the range of new compounds, and on the other hand, to enrich unique, uncharacteristic properties, such as boson peak [6] or structural, magnetic properties and low-temperature impedance behavior [7] in Ni_xInSe intercalates. Layered single crystals intercalated by foreign atoms of different nature allow the formation of nanostructured materials, so-called biintercalates [8, 9]. The formation of clathrate complexes on the basis of the mentioned single crystals of different complexity

with supramolecular guest component allows to realize quantum amplification of sensory sensitivity to external physical fields [10] and the fundamental possibility of storing electricity at the quantum level [11, 12].

A study of the conditions of thermodynamic advantage of biintercalation and the kinetic properties of biintercalates remains relevant. The important parameters of the observed phenomena are the structure and energy structure, relaxation time and electron scattering, conductivity and polarization. All these parameters will be determined mainly by the density of electronic states in the vicinity of ε_F. The corresponding change in thermodynamic parameters gives us an understanding of the conditions when biintercalation is energetically advantageous and on what microscopic parameters it depends.

Materials and research methods

A photosensitive quasi-two-dimensional gallium selenide semiconductor was selected as the host material (GaSe) [13], and sodium nitrite ($NaNO_2$) with ferric chloride ($FeCl_3$) were selected as ferroelectric and magnetoactive guest, respectively.

The formation of intercalate structures was carried out according to the intercalation technique described in [14, 15].

X-ray diffraction spectra were obtained on a diffractometer under CuK_α radiation monochromatized by reflection from the LiF monocrystal (200) planes, mounted on the primary beam, in a symmetrical θ–2θ scanning.

Impedance measurements were performed in the direction of the crystallographic C axis in the frequency range 10^{-3}–10^6 Hz using the AUTOLAB measuring system from Eco Chemie (Netherlands), equipped with computer programs FRA-2 and GPES. The removal of ambiguous points was performed by a Dirichlet filter [16, 17]. The frequency dependences of the complex impedance Z were analyzed by the graphoanalytical method in the environment of the software package ZView 2.3 (Scribner Associates). The approximation error did not exceed 4%. The adequacy of the constructed impedance models of the experimental data package was confirmed by the completely random nature of the frequency dependences of the residual differences of the first order [16, 17].

In order to determine the local energy levels, the thermally stimulated depolarization currents were measured.

Results and discussion

A biintercalate GaSe <$NaNO_2$+$FeCl_3$> was formed by the method of intercalation crystal engineering with ferroelectric guest components. The formation of this nanostructured biintercalate was carried out by the method of direct exposure of the original matrix first in sodium nitrite and then in iron trichloride. This process can be represented in the following sequence:

GaSe + $NaNO_2$ → GaSe<$NaNO_2$> (IV separation stage) + $FeCl_3$ → GaSe<$NaNO_2$+$FeCl_3$> (II separation stage).

The formation of intercalates proceeds not by the simultaneous occupation of all available "guest" positions but by the mechanism of "separation" [18, 19]. The formation of the fourth stage separation (GaSe<$NaNO_2$>) intercalate phases, and biintercalate of the second stage separation (GaSe<$NaNO_2$+$FeCl_3$>) occurred with a significant exothermic effect, indicating a covalent bond between the introduced guest content and the matrix. The structure of the obtained biintercatelate nanohybrid is schematically shown in Fig. 1.

Separation in the process of intercalation formation of biintercalate nanohybrid GaSe<$NaNO_2$+$FeCl_3$> leads to the emergence of a spatial-scale hybridity due to the alternation of nanoscale regions of meso- or microdimension phases. This is confirmed by the results of x-ray diffractometry, the spectra of which are presented in Fig. 2. Based on the analysis of the diffraction maximum profile (004), it can be seen that:

(i) As a result of intercalation modification, there is a shift of the angular maximum of the curves towards smaller scattering angles. It is also interesting to select an additional maximum for a biaterlate nanohybrid, which indicates the existence of two pronounced structures with two different distances between the layers. According to the Wolf–Bragg formula $d_{(hkl)} = \lambda / 2\sin\theta$ (λ = 1.5418 Å is the wavelength of CuK_α radiation), this result is due to an increase in the interplanar distance $d_{(004)}$ and, accordingly, the distance between the layers in the unexpanded packets of GaSe single crystals.

The value of the Bragg angle allows to determine the parameter c of the GaSe unit cell:

$$c = ld_{(hkl)} = 4d_{(004)}.$$

The parameters c of the experimental samples are presented in Fig. 2. It is noticeable that there is a pronounced tendency of the increase of the cell parameter c in the direction perpendicular to the layers of the single crystal,

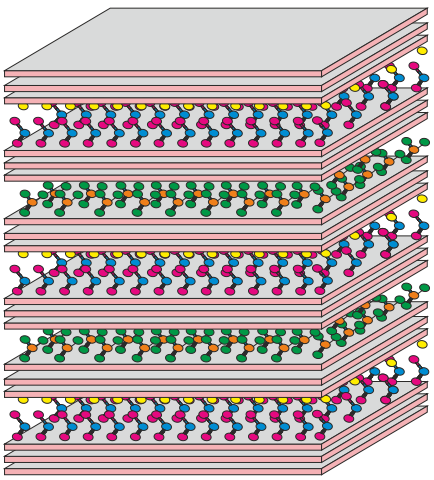

Fig. 1. (Color online) A schematic structure of a biintercalate nanohybrid GaSe<$NaNO_2$+$FeCl_3$>.

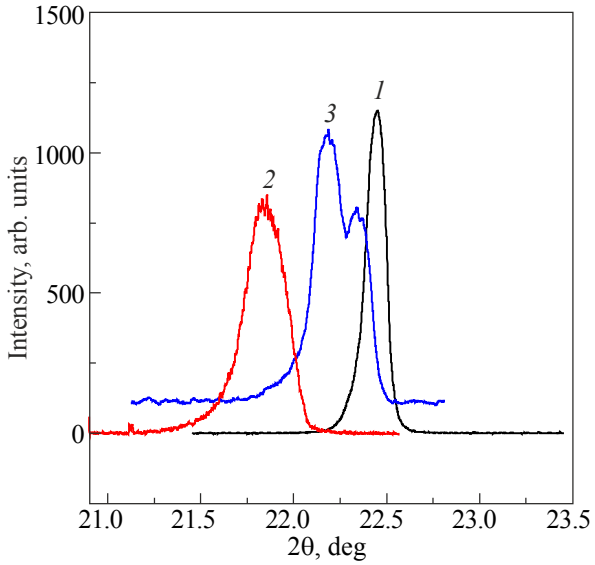

Fig. 2. X-ray diffractometry spectra for GaSe (*1*) (c = 15.917 Å), GaSe<$NaNO_2$> (*2*) (c = 16.2651 Å), and GaSe<$NaNO_2$+$FeCl_3$> (*3*) (c = 16.072, and 15.977 Å).

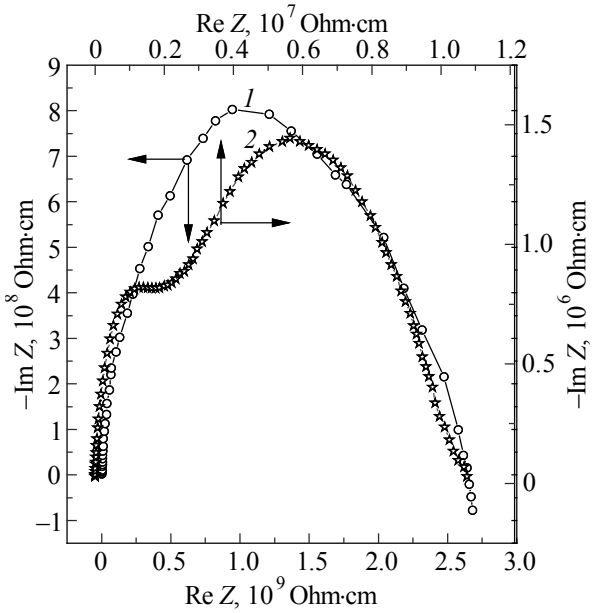

Fig. 3. Nyquist charts measured for the layered GaSe single crystals (*1*) and GaSe<$NaNO_2$+$FeCl_3$> biintercalate (*2*).

especially for the sample after 4-fold expansion with itercalated $NaNO_2$. In contrast, for the biintercalate there is not such a large increase in the cell parameter c, but there is an additional maximum, which indicates the existence of two structures with corresponding interplanar distances.

(ii) In addition to the displacement of the angular position of the Bragga maximum, there is also an increase in the half-width of the diffraction reflection curves compared to the original sample. According to the Wolf–Bragg formula,

$$\frac{\Delta d}{d} = -\operatorname{ctg}\theta\,\Delta\theta.$$

Thus, the extension of the reflection curves is proportional to the relative change in the interplanar distance, which indicates the presence of fluctuations in the distance between the layers in single crystals.

The results obtained for samples with different degrees of the hierarchy are well correlated. Intercalation of $NaNO_2$ has been found to form the intercalant phase of the fourth stage of separation and, at the subsequent biintercalation of $FeCl_3$, of the second stage one.

The next step was to study the conductive and polarizing properties of the biintercalate obtained by impedance spectroscopy method. In Fig. 3 shows Nyquist charts of layered GaSe single crystals and GaSe<$NaNO_2$+$FeCl_3$> biintercalate. In the case of layered GaSe single crystals, a single arc (Fig. 3, curve *1*), characterized by the current flow across the layers, is observed. On the other hand, for the biintercalate case, the Nyquist chart transforms and obtains a pronounced two-arc character (Fig. 3, curve *2*). In this case, the high-frequency arc represents the current flow through the unexpanded packages of the semiconductor matrix, and the low-frequency arc reflects the transfer of electric charge through the intercalated areas. An insertion of biintercalate guest component leads to the 250-fold increase in conductivity.

The represented experimental data show that biintercalation leads to significant physical changes in the internal matrix properties.

Even the simplest theoretical models of strongly anisotropic layered structures with staged ordering give good qualitative results.

In particular, according to [20], a model is proposed where the consideration of the electrons energy spectrum is limited to electronic states, which in the strong bond approach are formed by nondegenerate orbitals localized on atoms.

So, the electron subsystem is described by Hamiltonian, which takes into account the electron transfer between nodes within the layer, between the layers within the sandwich and between the sandwiches.

The sandwiches are divided by extended areas that can be considered as potential barriers. With increasing distance between sandwiches, the electron transfer between them decreases. That's why the studied system can be considered as a set of sequentially placed two-dimensional planes.

In this case, the electron density of states contains logarithmic divergence, typical for two-dimensional structures. It means that a twofold increase in the distance between sandwiches leads to the significant decrease in the electron transfer in this direction, as well as to a rebuilt electron density of states.

The increase in the electroconductivity of GaSe after biintercalation is caused by delocalized carriers and demonstrates the significant transformation of the intercalant energy spectrum and its dominant role in the current flow processes.

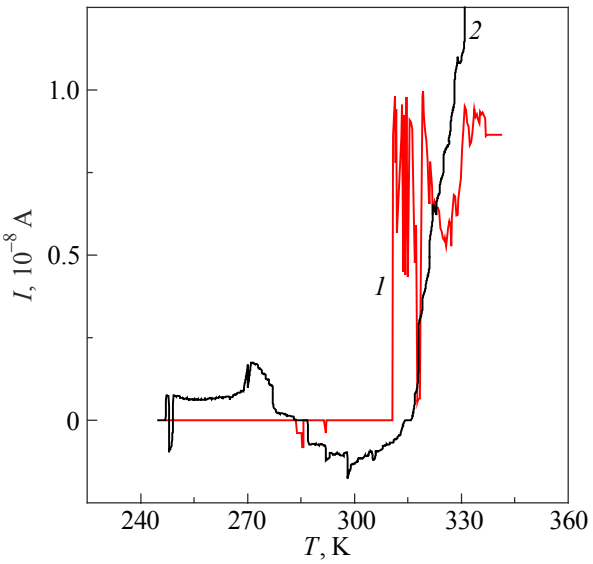

Fig. 4. Currents of thermaly stimulated discharge in the case of single GaSe (*1*) and biintercalated GaSe<$NaNO_2$+$FeCl_3$> (*2*).

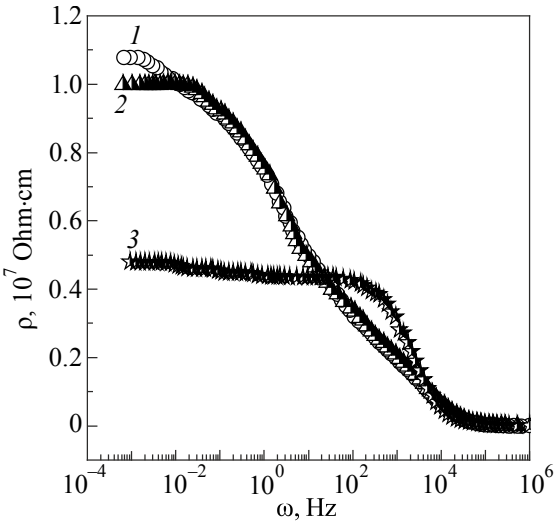

Fig. 5. Frequency dependences of the real component of the specific complex impedance perpendicular to the GaSe<$NaNO_2$+$FeCl_3$> nanolayers, measured under normal conditions (*1*), in the magnetic field (*2*) and under illumination (*3*)

To study energy spectrum of intercalant levels, the currents of a thermally stimulated discharge were measured in the case of single and biintercalated GaSe <$NaNO_2$+$FeCl_3$> (Fig. 4). In both cases relaxation of heterocharge is typical.

For a single-layer GaSe crystal, a local narrow band-energy spectrum is observed. The higher the temperature (above the room), the more the spectrum transforms to quasi-continuous one. On the other hand, for the biintercalate GaSe<$NaNO_2$+$FeCl_3$> the spectrum is quasi-continuous in all temperature region. The received result is in good agreement with the results of impedance spectroscopy.

Nyquist charts have a typical pattern reflecting the transfer of electric charge through unexpanded GaSe packets and potential barriers introduced by the biintercalant (Fig. 3, curve *2*).

The impedance studies at simultaneous action of light were carried out to reveal the effect of the ferroelectric guest on the conductive flow.

The measurements were performed under normal conditions, in a constant magnetic field (2.75 kOe), and under illumination (a simulator of solar radiation with a power of 65 W). Re Z is significantly reduced compared to the original GaSe matrix. A weak magnetoresistive effect was revealed at the lowest frequencies and the maximum of photosensitivity reaches ~ 2.5 times (Fig. 5).

It should also be noted that, under illumination, the behavior of Re $Z(\omega)$ reaches an independent frequency character in the wide frequency region, which is not inherent in the original unexpanded GaSe matrix. This result can be explained if we assume that the actual condition of the proximity of the host conduction zone and the filled band of states of guest content in the forbidden zone is realized during the biintercalation. Thus, when illuminated with white light, the energy will be enough to delocalize the main current carriers, which will cause an increase in the concentration of free carriers, i.e., the observed increase in conductivity in a fairly wide frequency range.

The dielectric constant shows an abnormal behavior (ε increases with increasing frequency in high-frequency region) for GaSe<$NaNO_2$+$FeCl_3$> biintercalate (Fig. 6). It is important to note that in this range the tangent of the dielectric loss angle takes values less than 1. In this case, this structure can be used to manufacture a high-capacity radio-frequency capacitor.

Polarization characteristics also behave in a usual way: the tangent of the angle of electric losses has a value of not less than 1 only in the high-frequency region ($\omega > 10^3$ Hz),

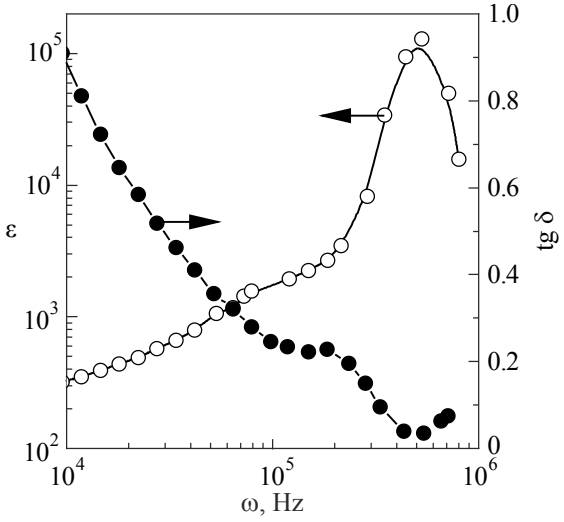

Fig. 6. Frequency dependences of the tangent of the angle of electric losses and dielectric constant for GaSe<$NaNO_2$+$FeCl_3$> biintercalate.

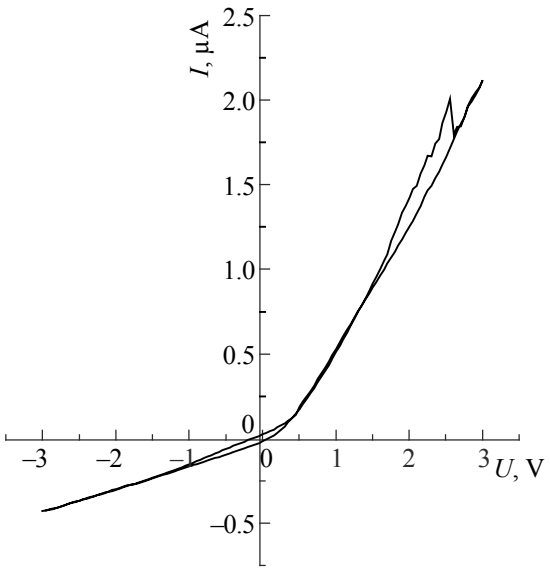

Fig. 7. Current-voltage characteristic of GaSe<$NaNO_2$+$FeCl_3$> under normal conditions.

in which the dielectric constant has the values typical for ferroelectric polarization (10^2–10^3). The presence of areas of anomalous dispersion on ε(ω) is invariable with respect to the type of host-guest interaction (Fig. 5).

Current-voltage characteristics show the accumulation of charge (which is typical for the nitrite-sodium encapsulates of gallium selenide), but it is not visualized in a magnetic field. Spin emf is not visible on the plot (Fig. 7).

The fact of «bending» of the *I–V* branches at $U = 0.44$ V, not at zero voltage, is interesting and still unclear.

Most likely, such *I–V* behavior is governed by a special condition of the electron subsystem, namely redistribution of charge carriers between nanoclusters in the deformation field.

Model and calculation

A special condition of the electron subsystem, namely redistribution of charge carriers caused by biintercalation, is studied in the virtual model crystal.

Layer crystals like GaSe belong to the strong anisotropic crystals, which can be described by a set of sandwiches connected by weak van der Waals interactions along the anisotropy axis. Each of these sandwiches consists of four covalent bonded Se–Ga–Ga–Se atomic planes. Such discrimination in chemical bonds causes an anisotropic electron energy spectrum, so-called Fivaz [21]:

$$(\boldsymbol{\chi}, k) = \alpha_c \chi^2 + t_c (1 - \cos k_z d), \tag{1}$$

where $\boldsymbol{\chi} = (a_x k_x, b_y k_y)$, $k_z \equiv k$, $\alpha = 1/2m^*_{x,y}$ ($m^*_{x,y}$ is the effective mass of an electron in the atomic plane within the sandwich), it is electron mixing between the nearest sandwiches along the anisotropic axis; $\hbar = 1$. The effective mass approximation is used to describe the electron within the sandwich (the Se–In–In–Se monoatomic *XOY* planes) and strong bond across the layers (along the anisotropy axis) in the nearest-neighbors approximation. Such energy law takes into account the different chemical bonds in different crystallographic directions of the layered crystal.

Two different types of guest atoms with corresponding average concentrations p_1 and p_2 are inserted in the van der Waals gap. The case of interacting layer GaSe single crystal and two different types of guest atoms is considered within the frame of virtual model crystal [22].

Subbands of electrons localized on corresponded guests are described by energy laws

$$\varepsilon_1(\mathbf{k}) = \alpha_1 \chi^2 + t_1 (1 - \cos d_z k_z) + \frac{\varepsilon_{01}}{p_1}, \tag{2}$$

$$\varepsilon_2(\mathbf{k}) = \alpha_2 \chi^2 + t_2 (1 - \cos d_z k_z) + \frac{\varepsilon_{02}}{p_2}. \tag{3}$$

The bottoms of the corresponding subbands are measured from ε_{0i}/p_i, where ε_{0i} is the energy of the ground state of corresponding intercalant with average concentrations p_i. The distinguishing of the nature of corresponding guest atoms is included through different energies ε_{01} and ε_{02} ($\varepsilon_{01} \neq \varepsilon_{02}$).

The Hamiltonian of biintercalate electron subsystem with inserted N_0 guest atoms of two types is built on the quantum function

$$\Psi(\mathbf{r}) = \sum_{\mathbf{n}} c_{\mathbf{nn}} \Psi(\mathbf{r}) + \sum_{\mathbf{n}} p_1(\mathbf{n}) a_{\mathbf{n}} \varphi_{1_{\mathbf{n}}}(\mathbf{r}) + \sum_{\mathbf{n}} p_2(\mathbf{n}) b_{\mathbf{n}} \varphi_{2_{\mathbf{n}}}(\mathbf{r}), \tag{4}$$

where summation is over all cells, $\psi_{\mathbf{n}}(\mathbf{r})$ is the wave function of an electron localized on the node of a layer crystal, $\varphi_{1,2_{\mathbf{n}}}(\mathbf{r})$ are a wave functions of an electron localized on the atom of intercalant of the 1st and 2nd type; probability

$$p_i(\mathbf{n}) = \begin{cases} 1, & \text{when in } \mathbf{n}\text{th node intercalant} \\ & \text{of the } i\text{th type is present,} \\ 0, & \text{when in } \mathbf{n}\text{th node intercalant} \\ & \text{of the } i\text{th type is absent.} \end{cases} \tag{5}$$

The Hamiltonian in the pulse approximation is

$$H = \sum_{\mathbf{k}} \varepsilon_c(\mathbf{k}) c^+_{\mathbf{k}} c_{\mathbf{k}} + p_1^2 \sum_{\mathbf{k}} \varepsilon_1(\mathbf{k}) a^+_{\mathbf{k}} a_{\mathbf{k}} + p_2^2 \sum_{\mathbf{k}} \varepsilon_2(\mathbf{k}) b^+_{\mathbf{k}} b_{\mathbf{k}} + p_1 \sum_{\mathbf{k}} V_1(\mathbf{k}) c^+_{\mathbf{k}} a_{\mathbf{k}} + p_2 \sum_{\mathbf{k}} V_2(\mathbf{k}) c^+_{\mathbf{k}} b_{\mathbf{k}} + \sqrt{p_1 p_2} \sum_{\mathbf{k}} V_{12}(\mathbf{k}) a^+_{\mathbf{k}} b_{\mathbf{k}} + \text{h.c.} \tag{6}$$

In Eq. (6), the dispersion laws are given by Eqs. (1)–(3), V_i describes the electron hybridization between *i*th intercalant subband and conductive band, and V_{12} describes the electron hybridization between different intercalant subbands.

The density of electron states was calculated using the equation of motion for corresponding retarded Green's functions $\left\langle\left\langle c_{\mathbf{k}} \middle| c_{\mathbf{k}}^{+}\right\rangle\right\rangle$, $\left\langle\left\langle a_{\mathbf{k}} \middle| a_{\mathbf{k}}^{+}\right\rangle\right\rangle$ and $\left\langle\left\langle b_{\mathbf{k}} \middle| b_{\mathbf{k}}^{+}\right\rangle\right\rangle$:

$$\left\langle\left\langle c_{\mathbf{k}} \middle| c_{\mathbf{k}}^{+}\right\rangle\right\rangle = \frac{\hbar}{2\pi}\frac{1}{D}\left\{\left(\hbar\omega\text{-}p_1^2\varepsilon_1\right)\left(\hbar\omega\text{-}p_2^2\varepsilon_2\right) - p_1p_2V_{12}^2 + \left(\hbar\omega-\varepsilon_c\right)\left(\hbar\omega - p_2^2\varepsilon_2\right) - p_2^2V_2^2 + \left(\hbar\omega-\varepsilon_c\right)\left(\hbar\omega - p_1^2\varepsilon_1\right) - p_1^2V_1^2\right\}, \quad (7)$$

$$\left\langle\left\langle a_{\mathbf{k}} \middle| a_{\mathbf{k}}^{+}\right\rangle\right\rangle = \frac{\hbar}{2\pi}\frac{1}{D}\left\{\left(\hbar\omega-\varepsilon_c\right)\left(\hbar\omega - p_2^2\varepsilon_2\right) - p_2^2V_2^2\right\}, \quad (8)$$

$$\left\langle\left\langle b_{\mathbf{k}} \middle| b_{\mathbf{k}}^{+}\right\rangle\right\rangle = \frac{\hbar}{2\pi}\frac{1}{D}\left\{\left(\hbar\omega-\varepsilon_c\right)\left(\hbar\omega - p_1^2\varepsilon_1\right) - p_1^2V_1^2\right\}, \quad (9)$$

where

$$D = \left(\hbar\omega-\varepsilon_c\right)\left[\left(\hbar\omega - p_1^2\varepsilon_1\right)\left(\hbar\omega - p_2^2\varepsilon_2\right) - p_1p_2V_{12}^2\right] + p_1V_1\left[-p_1V_1\left(\hbar\omega - p_2^2\varepsilon_2\right) - p_2\sqrt{p_1p_2}V_2V_{12}\right] - p_2V_2\left[p_2V_2\,2\left(\hbar\omega - p_1^2\varepsilon_1\right) + p_1\sqrt{p_1p_2}V_1V_{12}\right]. \quad (10)$$

Density of electron states

$$\rho(\omega) = -i\mathrm{Im}\left\{\left\langle\left\langle c_{\mathbf{k}} \middle| c_{\mathbf{k}}^{+}\right\rangle\right\rangle_{\omega+i\varepsilon} + \left\langle\left\langle a_{\mathbf{k}} \middle| a_{\mathbf{k}}^{+}\right\rangle\right\rangle_{\omega+i\varepsilon} + \left\langle\left\langle b_{\mathbf{k}} \middle| b_{\mathbf{k}}^{+}\right\rangle\right\rangle_{\omega+i\varepsilon}\right\}. \quad (11)$$

Particularly,

$$\rho(\omega) = A_1(\mathbf{k})\delta\left(\omega-\omega_1(\mathbf{k})\right) + A_2(\mathbf{k})\delta\left(\omega-\omega_2(\mathbf{k})\right) + A_3(\mathbf{k})\delta\left(\omega-\omega_3(\mathbf{k})\right), \quad (12)$$

where $\omega_i \in \{\omega_1,\omega_2,\omega_3\}$ energies are found as solutions of the equation $D(\hbar) = 0$:

$$A_i = \frac{Q(\hbar\omega_i)}{\left(\hbar\omega_i - \hbar\omega_j\right)\left(\hbar\omega_i - \hbar\omega_{j'}\right)}. \quad (13)$$

In Eq. (13) it $i \neq j \neq j'$ $Q(\hbar\omega_i)$ is an expression in curly brackets (9)–(11).

As shown in [22], in the case of $V_i = 0$, the resulted electron energy state of biintercalate has an additional gap in the density of states caused by the intercalant nature (value of $p_i e_{0i}$) and average concentrations p_i.

Electron density of state of the intercalate, including electron hybridization (V_1 = 0.12 eV, V_2 = 0.012 eV, V_{12} = = 0.05 eV), is shown below. Zero energy is measured from the bottom of the conductive band, and the width of forbidden gap is E_g = 2.1 eV, α_c = 1.0 eV, t_c = 0.1 eV.

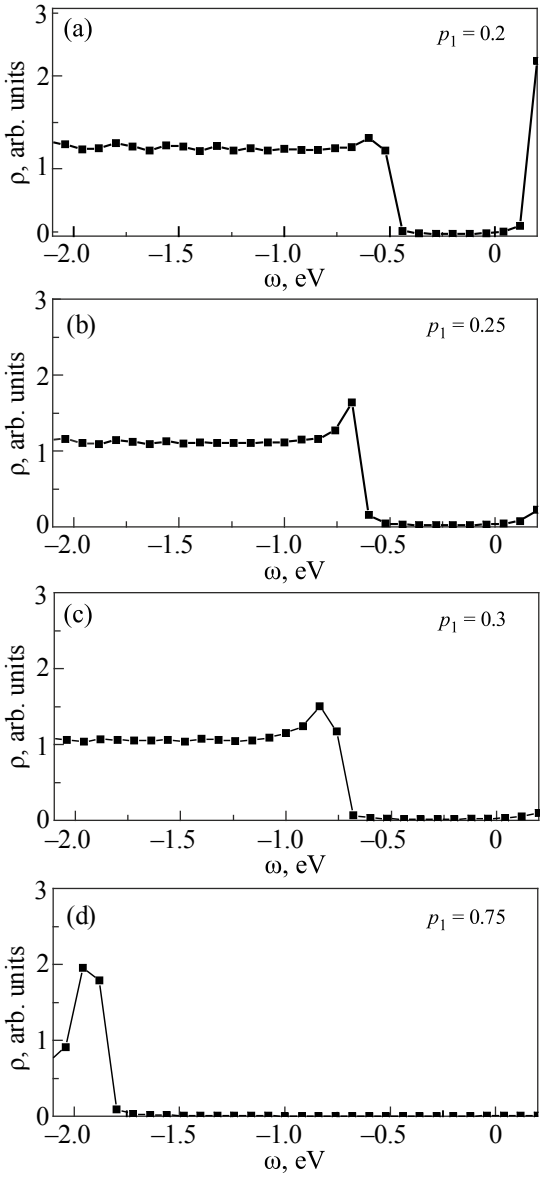

Fig. 8. Density of electron states of biintercalate at α_1 = –1.025 eV, t_1 = –0.1 eV, α_2 = 0.04 eV, t_2 = 0.04 eV, at different p_1 and p_2 = = 0.1 = const.

Calculations of GaSe biintercalate with intercalant-acceptor (ε_{01} = – 1.2 eV) and intercalant-donor (ε_{02} = – 0.2 eV) showed that:

(i) At fixed average concentration of the donor-type intercalant p_2 = const, the higher the average concentration of the acceptor-type intercalant p_1, the wider becomes the addition band (Fig. 8);

(ii) When the concentration of the donor-type intercalant increases (p_2), the additional gap becomes more narrow if p_2 rises (Fig. 9);

(iii) Calculations have shown that the smaller the anisotropy ($\alpha_i \approx t_i$), the narrower the additional gap.

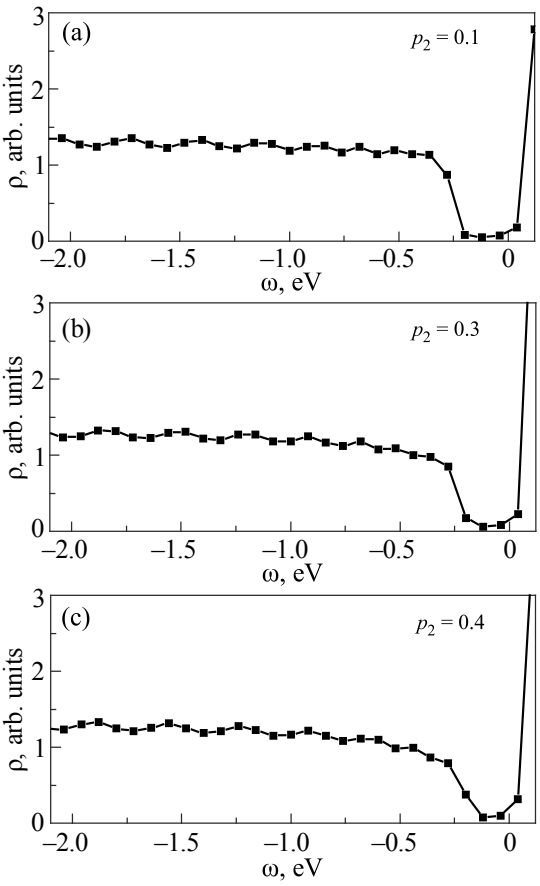

Fig. 9. Density of electron states of biintercalate at $\alpha_1 = -1.025$ eV, $t_1 = -0.1$ eV, $\alpha_2 = 0.04$ eV, $t_2 = 0.04$ eV, at different p_2 and $p_1 = 0.1 = \text{const}$.

Conclusions

During the formation of the GaSe<$NaNO_2$+$FeCl_3$> nanohybrid, due to separation in the process of intercalation formation of the biintercalate clathrate, there is a spatial-scale hybridity due to the alternation of nanoscale regions of one phase with meso- or microdimensions regions of the other.

The increase in the electrical conductivity of the GaSe matrix by 250 times after biintercalation is associated with delocalized carriers and indicates a significant transformation of the impurity energy spectrum and its predominant role in the processes of current passage. For the original GaSe single crystal, a local narrow-band character of the energy spectrum is observed, which turns into a quasi-continuous one at temperatures above room temperature. Instead, for the GaSe<$NaNO_2$+$FeCl_3$> biintercalant, the spectrum becomes quasi-continuous in the entire temperature range.

The dielectric constant of the GaSe<$NaNO_2$+$FeCl_3$> biintercalate in the high-frequency range reaches 10^5 at values of the dielectric loss angle tangent less than 1, which opens the prospect of using this nanostructure for the manufacture of high-capacity radio-frequency capacitor.

The current-voltage characteristics show the accumulation of charge, and the fact of «bending» of the *I–V* branches not at zero voltage but $U = 0.44$ V is interesting and is still unclear.

At low temperatures, the energy spectrum of biintercalate is found within the framework of the 3-band model: conductive band and two subbands formed by two types of intercalant. It is found that for biintercalate there is a violation of the density of states which mainly depends on parameter $\Delta = p_1\varepsilon_1 + p_2\varepsilon_2$. The conditions for which rising concentrations of the intercalant broaden the energy region and simultaneously significantly narrow the addition gap are studied.

1. J. Inarrea, *Appl. Phys. Lett.* **110**, 143105 (2017).
2. D. A. Bandurin, A. V. Tyurnina, G. L. Yu, A. Mishchenko, V. Zólyomi, S. V. Morozov, R. K. Kumar, R. V. Gorbachev, Z. R. Kudrynskyi, S. Pezzini, Z. D. Kovalyuk, U. Zeitler, K. S. Novoselov, A. Patanè, L. Eaves, I. V. Grigorieva, V. I. Fal'ko, A. K. Geim, and Y. Cao, *Nat. Nanotechnol.* **12**, 223 (2017).
3. I. Mora-Sero and J. Bisquert, *Nano Lett.* **6**, 640 (2006).
4. N. T. Hung, A. R. T. Nugraha, and R. Saito, *Appl. Phys. Lett.* **111**, 092107 (2017).
5. K. Geim and I. V. Grigorieva, *Nature* **499**, 419 (2013).
6. A. Baran, M. Botko, M. Kajňaková, A. Feher, S. Feodosyev, E. Syrkin, M. Klochko, N. Tovstyuk, I. Grygorchak, and V. Fomenko, *Fiz. Nizk. Temp.* **41**, 1191 (2015) [*Low Temp. Phys.* **41**, 930 (2015)].
7. Y. M. Stakhira, N. K. Tovstyuk, V. L. Fomenko, I. I. Grygorchak, A. K. Borysyuk, and B. A. Seredyuk, *Fiz. Nizk. Temp.* **38**, 69 (2012) [*Low Temp. Phys.* **38**, 54 (2012)].
8. Z. Chen, D. Guo, L. Si, and G. Xie, *Hindawi Scanning* **2017**, Article ID 9438573 (2017).
9. Y. Liang, H. D. Yoo, Y. Li, J. Shuai, H. A. Calderon, F. C. Robles Hernandez, L. C. Grabow, and Y. Yao, *Nano Lett.* **15**, 2194 (2015).
10. P. Chabecki, D. Całus, F. Ivashchyshyn, A. Pidluzhna, O. Hryhorchak, I. Bordun, O. Makarchuk, and A. V. Kityk, *Energies* **13**, 4321 (2020).
11. V. Maksymych , D. Całus, F. Ivashchyshyn, A. Pidluzhna, P. Chabecki, and R. Shvets, *Appl. Nanosci*. (2021) (In press).
12. I. Grygorchak, D. Calus, A. Pidluzhna, F. Ivashchyshyn, O. Hryhorchak, P. Chabecki, and R. Shvets, *Appl. Nanosci.* **10**, 4725 (2020).
13. *Preparation and Crystal Growth Material with Layered Structure*, R. M. A. Lies (ed.), Dordrecht, Boston (1977).
14. I. Grygorchak, F. Ivashchyshyn, P. Stakhira, R. R. Reghu, V. Cherpak, and J. V. Grazulevicius, *J. Nanoelectron. Optoelectron.* **8**, 292 (2013).
15. T. M. Bishchaniuk, O. V. Balaban, R. Y. Shvets, I. I. Grygorchak, A. V. Fechan, B. A. Lukiyanets, and F. O. Ivashchyshyn, *Mol. Cryst. Liq. Cryst.* **589**, 132 (2014).

16. Z. B. Stoinov, B. M. Grafov, B. S. Savova-Stoinova, and V. V. Elkin, *Electrochemical Impedance*, Nauka, Moscow (1991).
17. *Impedance Spectroscopy. Theory, Experiment and Application*, E. Barsoukov and J. R. Macdonald (eds.), Wiley-Interscience, Hoboken (2005).
18. S. A. Safran, *Solid State Physics: Adv. Res. and Appl*. **40**, 246 (1987).
19. I. I. Grigorchak, V. V. Netyaga, S. V. Gavrilyuk, B. P. Bakhmatyuk, and Z. D. Kovalyuk, *Phys. Solid State* **43**, 1442 (2001).
20. I. V. Stasyuk and O. V. Velychko, *J. Phys. Studies* **18**, 2002 (2014) (In Ukrainian).
21. R. F. Fivaz, *J. Phys. Chem. Solids* **28**, 839 (1967).
22. N. K. Tovstyuk, *Visnyk of the Lviv University. Ser. Physics* **48**, 109 (2013) (In Ukrainian).

Біінтеркалатна шарувата гетероструктура: умови синтезу та фізичні властивості

F. O. Ivashchyshyn, V. M. Maksymych, T. D. Krushelnytska, O. V. Rybak, B. O. Seredyuk, N. K. Tovstyuk

Реалізовано біінтеркаляцію шаруватого напівпровідника GaSe сегнетоелектричним та феромагнітним гостьовими компонентами. За рахунок ешелонування гостьових компонентів наногібрид GaSe<$NaNO_2$+$FeCl_3$> володіє просторово-масштабною гібридністю, яка зумовлена чергуванням нанорозмірних областей однієї фази з мезо- чи мікророзмірними іншої. Результати досліджень електропровідності методом імпедансної спектроскопії свідчать про 250-кратне її зростання після біінтеркаляції монокристалу GaSe, що зумовлено делокалізованими носіями струму. Підтвердження суттєвої зміни домішкового енергетичного спектру після біінтеркаляції отримано методом термостимульованого розряду — наногібрид GaSe<$NaNO_2$+$FeCl_3$> характеризується квазінеперервним спектром у всій температурній області вимірювань та релаксацією гетерозаряду. Наногібрид GaSe<$NaNO_2$+$FeCl_3$> характеризується високим значенням діелектричної проникності при тангенсі кута діелектричних втрат меншому за 1 у високочастотній області спектру, що відкриває перспективу його використання для виготовлення високодобротних радіочастотних конденсаторів. Зміни домішкового енергетичного спектру досліджуються у випадку низьких температур в моделі віртуального кристалу з врахуванням фівазівського закону дисперсії як для зони провідності, так і для двох домішкових зон. Встановлена поява додаткової щілини в спектрі домішкових станів та досліджується її зміна залежно від концентрації різних за природою інтеркалянтів — акцепторного типу та донорного.

Ключові слова: біінтеркаляція, шаруватий кристал, нанорозмір, наногібрид, віртуальна модель.